University of Salford
Materials & Physics Research Centre

Novel White Light Lasers

C S Rose, G S McDonald and J M Christian

Materials & Physics Research Centre, University of Salford, UK

Abstract **We report on detailed investigations of a novel self-organisational effect that can convert laser light into an extremely broad comb of multi-colour beams. The importance of this new effect is that it spontaneously gives rise to an extreme enhancement of the output comb bandwidth, and that constituent frequencies may self-synchronize.**

Introduction

Lasers typically emit light of one or two, well-defined, frequencies (or 'colours'). However, numerous applications arise if such light can be converted into a broad, multi-frequency (e.g. 'multi-colour') comb of laser beams. Applications range from meteorology, sensing and measurements to those potentially in the domain of the emerging research field of Attosecond Science.

Here, we report on a new effect that gives rise to an output laser bandwidth (spectral width) that may extend across the entire visible spectrum, resulting in **White Light Laser output**. The breadth of new frequencies actually extends well beyond this – into the invisible infra-red and ultra-violet regions of the electromagnetic spectrum. The synchronization of so many frequencies can result in Attosecond pulses.

There have been several reports of contexts [1-3] where efficient broadband frequency comb generation may be possible. We will demonstrate distinctiveness with regard to these known contexts, and summarise results from an exhaustive exploration of this new effect.

Configuration

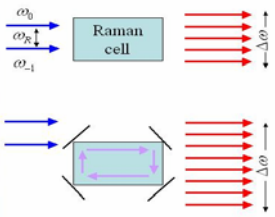

Fig 1: Schematic of non-cavity and cavity Raman systems

Model

Our most recent work has considered a new fundamental modification to the Raman process: through the inclusion of cavity feedback effects (see Fig 1). A steady state model can be obtained from the fully-transient equations by considering pump pulses whose duration t_p is much longer than the characteristic dephasing time, T_2, of the medium polarisation P. This consideration ($t_p >> T_2$) allows one to neglect the polarization dynamics - so that each (normalized) **electric field envelope A_n for the nth frequency component evolves in distance Z according to:**

$$\frac{dA_n}{dZ} = \frac{\omega_n}{2\omega_0}\left[P^* A_{n+1}\exp(-i\gamma_{n+1}Z) - P A_{n-1}\exp(i\gamma_n Z)\right],$$

$$P = \sum_j A_j A_{j-1}^* \exp\left(-i\gamma_j Z\right)$$

where $\omega_n = \omega_0 + n\omega_R$ is the frequency of the nth Raman sideband, ω_0 is the pump frequency, ω_R is the Raman transition frequency. The dimensionless propagation length is $Z = g I_0 z$, where g is the gain coefficient of the transition and I_0 is the pump peak intensity. The set of normalized mistuning's is given by $\gamma_n = \Delta_n / g I_0$, where $\Delta_n = (k_n - k_{n-1}) - (k_0 - k_{-1})$. The above governing equations are then supplemented by **ring-cavity boundary conditions**: the pump (n = 0) and first Stokes (n = -1) field envelopes satisfy

$$A_0(0) = 1 + R(\omega_0)\exp(i\phi_0)A_0(Z_C) \qquad A_{-1}(0) = 1 + R(\omega_{-1})\exp(i\phi_{-1})A_{-1}(Z_C)$$

while all other fields are subject to

$$A_n(0) = R(\omega_n)A_n(Z_C).$$

Here, **Z_C is the normalized cavity length** and $R(\omega_n)$ are the frequency-dependent reflectivity coefficients. Normalised cavity mistunings ϕ_0 and ϕ_{-1} are required for only the pump and first Stokes fields since there is no external driving of (i.e. no phase reference for) the other frequency components.

Results

Fig 2: Output Spectral Width Generated (long-term)

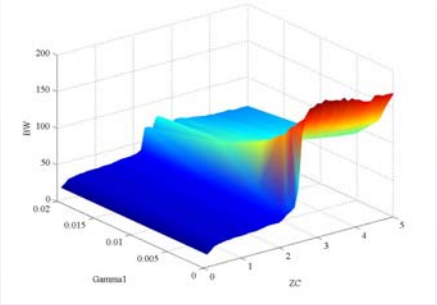

Figure 2: A surface plot of Spectral bandwidth vs. Medium dispersion (Gamma1) and Cavity length (Z_C) parameters. Values of spectral bandwidth are taken as averages over a long-term period of over 1000 cavity transits. As can be seen from this figure there is a **substantial increase in bandwidth over the non-cavity contexts** (which result in only up to 50 frequencies). We find that, at above a value of around Z_C = 2.5, there is a step increase in the number of new frequencies generated (well in excess of 100 components result). We also find that at higher levels of dispersion (values greater than 0.005), spectra are unaffected by dispersion level and bandwidth is comparable to the non-cavity case. We have considered a **moderate reflectivity** of R=0.9 and discover that **longer cavities ultimately result in the widest spectral output**. Maximum bandwidth is predicted when medium dispersion is low.

Fig 3: Initial Spectral Growth (in terms of cavity reflectivity and cavity length)

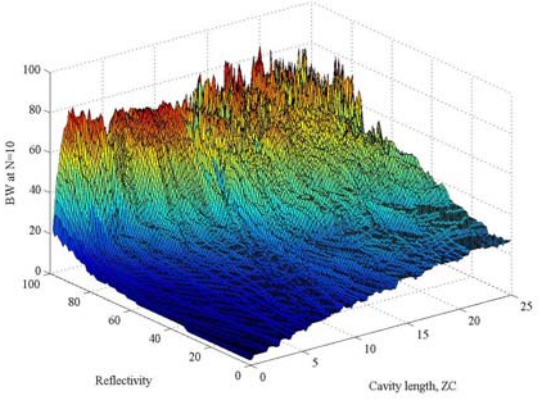

Figure 3: A surface plot of Bandwidth vs. Reflectivity and Z_C parameters with a fixed finite dispersion value, The bandwidth is taken at transit number N = 10. This data shows how the values of reflectivity and cavity length effect the bandwidth during the initial growth of the spectrum. It is clear to see from the figure that an increase in reflectivity or cavity length more rapidly generates bandwidth, therefore inferring that the rate of bandwidth growth are related to both the reflectivity and cavity length. As the reflectivity reaches the extreme value of R=0.99 the change in growth due to increasing cavity length is found to be subdued.

Fig 4: Initial Spectral Growth (in terms of medium dispersion and cavity length)

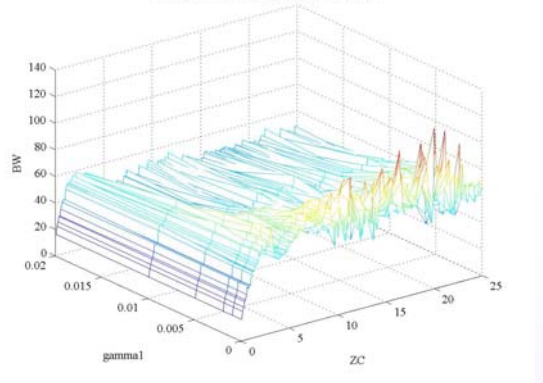

Figure 4: A surface plot of Bandwidth vs. Medium dispersion (gamma1) and Cavity length (Z_C) parameters. As in Figure 3, bandwidth is noted after at a fixed number of cavity transits (N = 10). It can clearly be seen that, at dispersion values greater than 0.005, the effect of dispersion on initial spectral bandwidth is minimal. Again, the value of initial bandwidth generated **increases with increasing cavity length** until it reaches a steady value (Z_C > 4), after which increases in cavity length produce little change to the initial bandwidth growth rate. This is in agreement with Figure 3. Data is shown here for R=0.9. Increasing reflectivity towards higher values (such as R=0.99) decreases the value of cavity length required to reach a steady value of bandwidth. Hence, the initial growth rate of the system at moderate to high reflectivities is unaffected by greatly increasing cavity length – this is in direct contrast to the long-term bandwidth, shown in Figure 2, which depends strongly on cavity length.

Conclusions

Broadband multiline frequency combs present a wealth of applications, ranging from meteorology, sensing and measurements to those potentially in the domain of attosecond science. Over the last decade, there have been several reports of cavity contexts where efficient broadband multiline generation is possible. These contexts include spherical micro-cavities [1], monolithic microresonators [2] and so-called 'bottle micro-resonators' [3], in which the cavity quality to mode volume ratio (Q / V) plays a dominant role in the characteristics of the device and its constituent whispering gallery modes. Typically, maximum quality and low volume lead to the optimal condition of high Q / V.

We have reported on detailed investigations of a **novel Raman self-synchronous process that is accompanied by extreme enhancement of the bandwidth** of the generated frequencies. To illustrate distinctiveness from these well-known contexts, we have stressed that **the effects we report can be optimal in low-Q resonators: i.e. either cavities with very moderate reflectivities; or in larger volume cavities** (e.g. for longer cavity lengths).

Work is underway to use the above data to construct semi-analytical models of the underlying mechanisms involved in this new broadband light generation process.

References: [1] Spillane S M, Kippenberg T J and Vahala K J, *Nature* **415,** 621 (2002).
[2] Del'Haye P *et al, Nature* **450,** 1214 (2007).
[3] Pollinger M *et al, Phys. Rev. Lett.* **103,** 053901 (2009).

Contact: Christopher Rose, Maxwell room 114, University of Salford, Salford, UK, M5 4WT.
email: c.s.rose@pgr.salford.ac.uk